CHEMISTRY
AN ASIAN JOURNAL
www.chemasianj.org

Accepted Article

Title: Aggregation behaviour of non-ionic twinned amphiphiles and their application as biomedical nanocarriers

Authors: Abhishek K. Singh, Bala N. S. Thota, Boris Schade, Katharina Achazi, Abdullah Khan, Christoph Böttcher, Sunil K. Sharma, and Rainer Haag

To be cited as: *Chem. Asian J.* 10.1002/asia.201700450

Link to VoR: http://dx.doi.org/10.1002/asia.201700450

A Journal of

ACES
Asian Chemical Editorial Society

A sister journal of **Angewandte Chemie** and **Chemistry – A European Journal**

WILEY-VCH

10.1002/asia.201700450

WILEY-VCH

Aggregation behaviour of non-ionic twinned amphiphiles and their application as biomedical nanocarriers

Abhishek K. Singh[a], Bala N. S. Thota[b], Boris Schade[c], Katharina Achazi[b], Abdullah Khan[a], Christoph Böttcher* [c], Sunil K. Sharma*[a], Rainer Haag*[b]

Abstract A new class of twinned amphiphiles was developed by conjugating a pair of hydrophilic head groups from mPEG chains (Mn: 350 or 1000) and a pair of hydrophobic segments from linear alkyl chains (C_{11} or C_{18}) through a novel spacer synthesized from glycerol and *p*-hydroxybenzoic acid. The aggregation phenomena of the amphiphiles were proven by DLS and fluorescence experiments, whereas size and morphology of the aggregates were evaluated by cryo-TEM, the measurements proved the formation of globular, thread-like or rod-like micelles as well as planar double-layer assemblies, depending on the amphiphile's molecular structure. The applicability of these non-ionic amphiphilic systems as nanocarriers for hydrophobic guest molecules was demonstrated by encapsulating a hydrophobic dye, Nile red, and a hydrophobic drug, Nimodipine. The transport capacity results for both Nimodipine and Nile Red prove them as a promising candidate for drug delivery.

Introduction

Self-assembly of amphiphilic molecules is a prevalent principle of nature to construct functional entities covering diverse phenomena like protein folding, compartmentalization, and information transcription. Although amphiphilic molecules have been studied for decades to understand their physicochemical properties and aggregation behaviour, only recently controlled architectures are studied for potential applications for drug / gene delivery and in optoelectronics among others.[1,2,3] So far, a large number of amphiphilic systems have been developed and investigated for their self-assembly into a wide variety of nanostructures.[4,5] However, these can be broadly divided into two major classes each comprising its own advantages. While polymeric amphiphiles (PA) result in more stable nanostructures, small molecule amphiphiles (SMAs) are more simple in design and their self-assemblies displays more similarity with the natural analogs.[6-10] Recently, Zhu *et al.* developed a drug self-delivery system for cancer therapy by synthesizing amphiphilic drug-drug conjugate.[11]

Among SMAs, Gemini amphiphiles have attained considerable attention, due to their superior physicochemical properties such as low critical aggregation concentration (CAC) and the formation of stable aggregates.[12-14] The influence of different molecular parameters on the aggregation behaviour of Gemini amphiphiles is well reported in the literature[15,16] and the knowledge of such dependencies has been utilized for the design of novel carriers in biomedical applications, particularly in gene delivery as most of the Gemini amphiphiles reported so far are cationic in nature.[17-19] There are, however, only few reports available describing their applications as nanocarrier for the delivery of hydrophobic drug molecules. A major reason for this may be that the cationic Gemini amphiphiles are known to acquire cytotoxicity[20] while particularly non-ionic amphiphiles are advantageous for drug delivery applications.[21,22] Non-ionic Gemini amphiphiles based on carbohydrates have been well studied in literature.[23-26] However, our interest is to explore the use of other competing moieties to come up with an amphiphilic system with an improved capacity for drug delivery. In this respect, polyethyleneglycol (PEG) is considered as a potential choice due to its specific properties, such as water solubility, non-toxicity, decreased interaction with blood components, good chemical stability, and biocompatibility. Implementing non-ionic PEG as the hydrophilic building block of Gemini amphiphiles provides a new type of amphiphiles featuring the beneficial characteristics of pegylation like biocompatibility, reduced immunogenicity and antigenicity, as well as prolonged circulation by reduced renal clearance.[27,28] The availability of PEG in a broad range of molecular weights is additionally advantageous to fine-tune the properties of the such amphiphiles. Although the physicochemical behaviour of PEG-based Gemini amphiphiles has been studied before[29-31], only few such molecules have been applied as nanocarriers for hydrophobic molecules.[32,33]

To expand the scope of such systems for drug delivery applications, we have synthesized a series of new non-ionic amphiphilic compounds (**1**-**4**) (**Figure 1**), which are constituted from two hydrophilic (mPEG) and two hydrophobic (alkyl chain)

[a] Abhishek K. Singh, Abdullah Khan, Prof. Sunil K. Sharma
Department of Chemistry, University of Delhi, Delhi, India
E-mail: sksharma@chemistry.du.ac.in
[b] B.N.S. Thota, Dr. Katharina Achazi, Prof. Rainer Haag
Institut für Chemie und Biochemie, Freie Universität Berlin, Takustraße 3, 14195 Berlin, Germany
E-mail: haag@zedat.fu-berlin.de
[c] Dr. Boris Schade, Dr. Christoph Böttcher
Forschungszentrum für Elektronenmikroskopie, Institut für Chemie und Biochemie, Freie Universität Berlin, Fabeckstraße 36a, 14195 Berlin, Germany
E-mail: christoph.boettcher@fzem.fu-berlin.de

Supporting information for this article is given via a link at the end of the document. ((Please delete this text if not appropriate))

moieties connected via a triazolyl *p*-hydroxybenzoate spacer (**Scheme 1**). This is the first report of using such an A_2B_2 spacer moiety with aromatic and non-aromatic units that may enhance the solubilization and encapsulation potential of the synthesized amphiphilic units for hydrophobic cargo delivery.[21,34] We termed the compounds twinned because they do not exactly fit to the definition of Gemini amphiphiles, having a slightly different arrangement of the paired hydrophobic and hydrophilic segments around the shared spacer.[35]

The new amphiphiles were characterized with respect to their assembly behaviour by using fluorescence, dynamic light scattering (DLS), and cryogenic electron microscopy (cryo-TEM). Furthermore, their application as nanocarriers for hydrophobic guests is demonstrated by using two established standards, the hydrophobic dye Nile red and the hydrophobic drug Nimodipine.

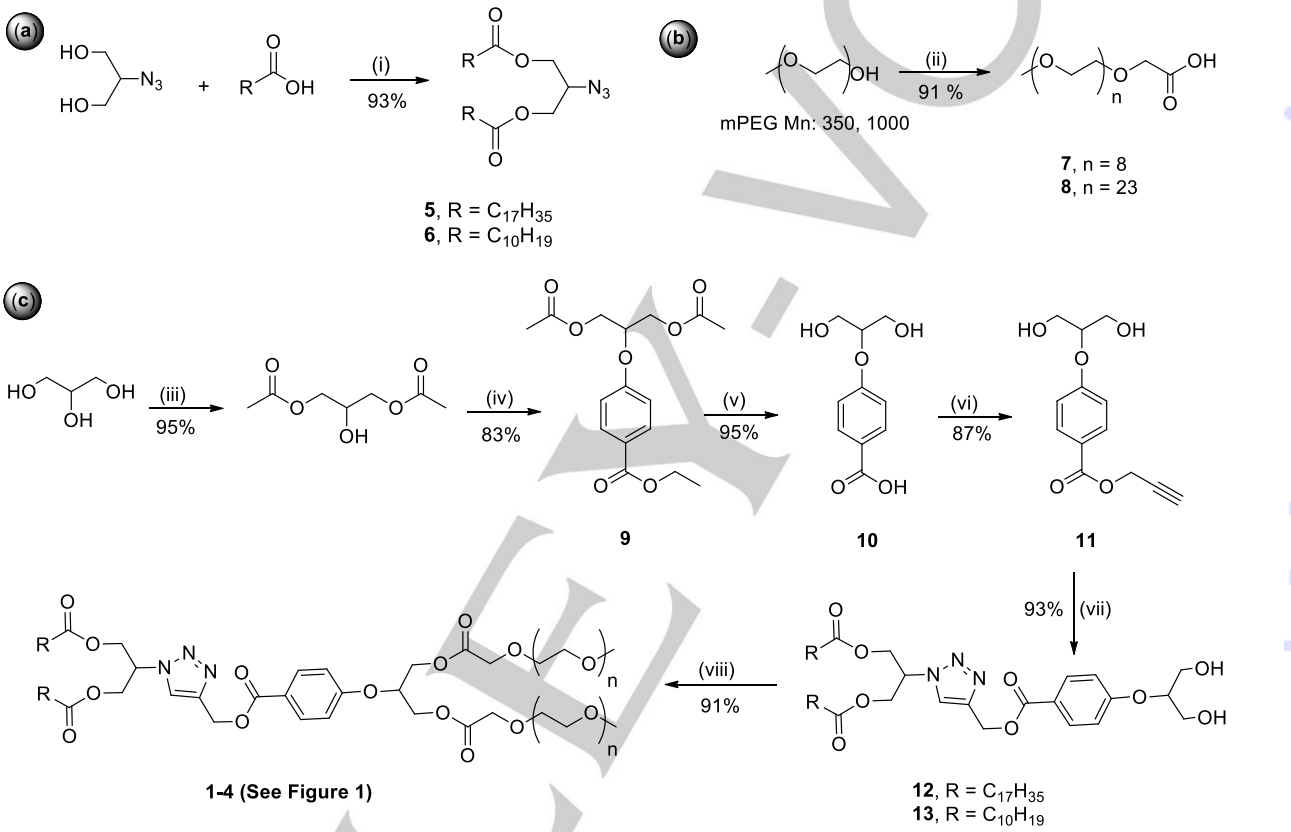

Scheme 1. Synthesis of mPEG based non-ionic twinned amphiphiles: a(i) EDC.HCl, DMAP, DCM, 15 h, 30 °C; b(ii) $KMnO_4$, NaOH, water, 24 h 80 °C; c(iii) Novozym 435, vinyl acetate, THF, 2 h, 30 °C; (iv) ethyl 4-hydroxybenzoate, DIAD, TPP, THF, 15 h, 30 °C; (v) 1N NaOH in methanol, water, 4 h, 50 °C; (vi) propargyl bromide, K_2CO_3, DMF, 6 h, 60 °C; (vii) compound **5**/**6**, sodium ascorbate, copper sulphate, THF:water (3:1), 15 h, 50 °C; (viii) compound **7**/**8**, EDC.HCl, DMAP, DCM, 15 h, 30 °C.

Results and Discussion

Synthesis

The aggregation behaviour of amphiphilic system depends on several factors such as the length of the different structural constituents (hydrophilic, hydrophobic moieties and spacer). To investigate the influence of the size of the hydrophobic alkyl moiety and the chain length of the hydrophilic mPEG group on the aggregation behaviour, we have synthesized four twinned amphiphiles (**1**-**4**) by varying the alkyl (C_{18} or C_{11}) and mPEG (Mn: 350 or 1000) chain lengths (**Scheme 1**). All of these amphiphiles were synthesized starting from glycerol which was first converted to 2-hydroxypropane-1,3-diyl diacetate using vinyl acetate as the acylating reagent, by following the established bio-catalytic procedure.[36] The secondary hydroxyl group of 2-hydroxypropane-1,3-diyl diacetate was then coupled with 4-hydroxybenzoate *via* Mitsunobu reaction.[37] The resulting compound **9** was characterized from its spectral data. In its ^{1}H NMR spectrum, the methine (-OC*H*(CH_2O-)$_2$) protons get deshielded and appear at δ 4.79-4.75 as compared to the

precursor glycerol 1,3-diacetate (δ 4.1). Hydrolysis of the product with methanolic NaOH solution yielded compound **10**. The characteristic signals for the acetyl moiety i.e. the singlet at δ 2.06 in ^{1}H NMR and the peaks at δ 20.86, 170.79 in the ^{13}C NMR spectra in compound **9** disappeared completely upon hydrolysis. Compound **10** was further subjected to selective propargylation at the carboxylic site to obtain the desired *p*-hydroxybenzoate spacer **11**. This compound was characterized on the basis of its ^{1}H-NMR spectrum, the methylene (-C*H*$_2$C≡CH) and methine (-CH$_2$C≡C*H*) protons of the propargyl moiety appear at δ 4.86 and 2.50, respectively. Diacyl 2-azido glycerol (**5**/**6**) was then "Click" coupled at the propargyl end of the spacer forming compounds **12** and **13**. Finally, mPEG acid (**7**/**8**) was linked to the diol (**12** /**13**) *via* esterification to obtain the targeted twinned amphiphiles (**1**-**4**) (**Scheme 1**). Characterization of these amphiphiles using ^{1}H- and ^{13}C-NMR, IR, and gel permeation chromatography (GPC) (**Figure 1**) unambiguously validated their intended structure. The characteristic triazolyl ring protons appear in the range δ 7.77-7.78 in the ^{1}H NMR spectra, while the methylene protons neighbouring the triazole ring appear at δ 5.0-5.5 ppm. The molecular weight and PDI for all of the resultant amphiphiles (**1**-**4**) obtained from GPC are listed in the **Figure 1**.

Aggregation behaviour

Four different non-ionic twinned amphiphiles (**1**-**4**) synthesized by varying the ratio of hydrophilic and hydrophobic moieties were observed to exhibit variation in solubility and aggregation behaviour in aqueous medium. Amphiphiles **3** and **4** having larger mPEG (Mn: 1000 g/mol) turned out to be more soluble in water as compared to **1** and **2** with smaller mPEG units (Mn: 350 g/mol), this behaviour can be quantified by the Griffin method of evaluating the hydrophilic-lipophilic balance (HLB) for non-ionic surfactants (see **Figure 1**).[38] The aggregation behaviour of the amphiphiles (**1**-**4**) was studied in aqueous solution by fluorescence spectroscopy, dynamic light scattering (DLS), and cryogenic electron microscopy (cryo-TEM). The CAC of amphiphiles was measured by fluorescence spectroscopy using pyrene as a probe. In general, the emission spectrum of pyrene displays a well-defined vibronic structure. The intensity of the first and third vibronic peaks is considerably sensitive to the polarity of the surrounding medium and their ratio is a good measure for the microenvironment of the fluorophore.[39] In our typical experimental setup, a stock solution of pyrene (0.5 mM) in Milli Q water was prepared and the pyrene stock solution was used to prepare different samples of the amphiphiles with

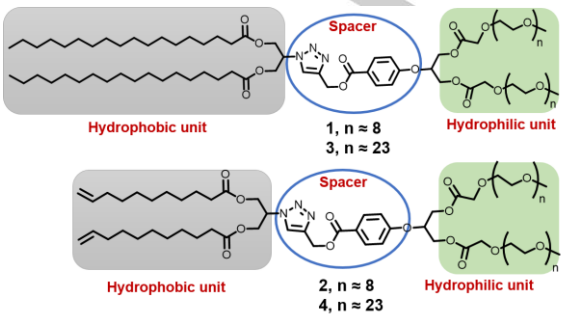

Amphiphiles	[a] MW [g mol^{-1}]	PDI	[b] Mh [g mol^{-1}]	[c] HLB = 20 x Mh / MW
1	1979	1.03	700	7.0
2	1513	1.03	700	9.2
3	2555	1.18	2000	15.6
4	2339	1.19	2000	17.1

a = Molecular weight of amphiphiles determined by GPC, b = Molecular weight of hydrophilic part
c = Griffin equation

Figure 1. Calculation of HLB value using Griffin equation.

required concentrations. All the solutions were filtered using 0.22 µm polytetrafluoroethylene (PTFE) filter to remove the non-encapsulated dye. The fluorescence spectra were recorded at 20 °C for the filtered clear solutions and from the fluorescence intensity data, I_1 (λ_1: 372 nm) and I_3 (λ_3: 385 nm), the ratio of I_3/I_1 was calculated and plotted with the log [amphiphile concentration] to obtain the CAC values (**Figure 2)**. Since the amphiphile **1** has limited solubility in aqueous medium, the CAC values were recorded for amphiphiles **2**, **3** and **4** only.

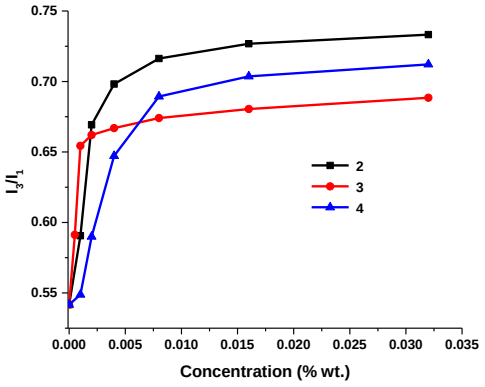

Figure 2: Determination of the critical aggregation concentration of amphiphiles **2**-**4** using fluorescence spectroscopy and pyrene as a probe.

Amphiphile **3** constituted from larger hydrophobic (C_{18} alkyl chain) and hydrophilic (mPEG Mn: 1000) groups was found to have lowest CAC value of 0.7 x 10^{-5} M. However, reducing the size of hydrophobic alkyl chain (C_{11}) increases the CAC by two fold in amphiphile **4** with a value of 1.4 X 10^{-5} M. On the other

hand reducing the size of both, hydrophobic (C_{11}) and hydrophilic (mPEG Mn: 350) groups enhances the CAC value significantly to 4.8 x 10^{-5} M.

The size of the aggregates was determined by dynamic light scattering (DLS) measurements. For amphiphiles **1**-**3,** DLS displayed unimodal size distribution of the formed aggregates with diameters of around 85, 53, and 98 nm, respectively, while the least hydrophobic compound **4** exhibited a bimodal intensity profile with peaks at 11 and 125 nm. Corresponding plots of the volume distribution displaying values of 53, 35, 40 and 9 nm for amphiphiles **1**, **2**, **3** and **4**, respectively (**Figure 3**), clearly indicate that smaller aggregates represent the majority of entities present within the samples.

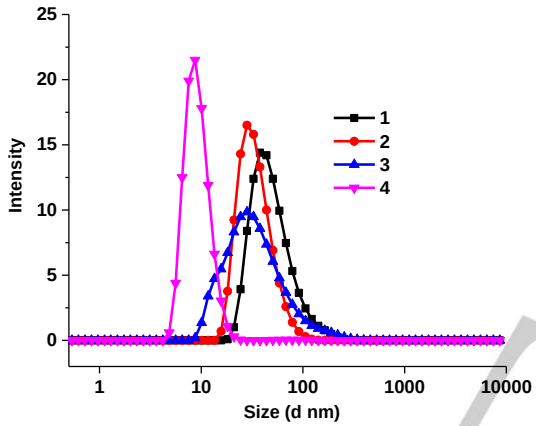

Figure 3: DLS profile for the amphiphiles **1**-**4** in water.

Cryo-TEM

The morphology of the twinned amphiphiles aggregates was studied in aqueous solutions using cryogenic transmission electron microscopy (cryo-TEM). All samples were prepared according to our standard preparation protocol (see SI). Since amphiphile **1** has limited solubility in pure water, self-assembly of this compound was investigated in the presence of small amount of THF (2.5% v/v). At an amphiphile concentration of 0.25 wt%, individual aggregates could hardly be distinguished due to the dense packing. At reduced concentration of 0.125 wt% individual flat and also twisted ribbons of several 100 nm in length could be identified (**Figure 4**). In some cases flat ribbons present their side views with a typical bilayer density profile of about 8 - 9 nm thickness (black-rimmed arrowhead). Twisted ribbons, which occasionally occur, provide sequences of high-contrast side views and low contrast top views (white arrowheads). As this latter morphology reflects the different orientation at a 360° turn it clearly identifies the ribbon-like nature of the assemblies. Broader ribbons indicate a more pronounced tendency towards lateral growth instead of stacking (black arrowhead). Sometimes they widen in a stepwise manner, suggesting their construction from side by side arranged narrow ribbons. (see also SI for TEM micrographs of negatively stained samples).

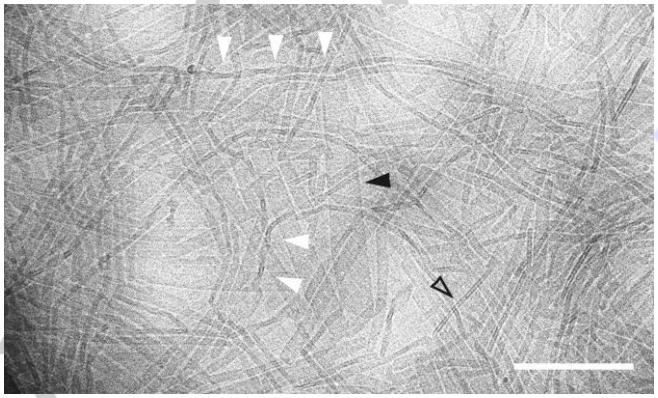

Figure 4. Cryo-TEM micrograph of amphiphile **1** at a concentration of 0.125 wt%. Planar ribbons of different width and length dominate the preparation (black arrowhead) and occasionally provide their contrast bilayered side views (black-rimmed arrowheads).Twisted entities (white arrowheads) identify the complete morphology of the assemblies. Bar is 200 nm.

Both amphiphiles **2** and **3** form elongated assemblies in aqueous solutions (**Figure 5**). Amphiphile **2** self-assembles into flexible threads with diameters ranging from 4.7 to 5.5 nm which appear as individual aggregates even at a concentration as high as 0.5 wt%. Dark spots along the course of the threads represent top views of sections that are situated perpendicular to the embedding ice film.

Samples of amphiphile **3** showed individual assemblies only at concentrations of 0.125 wt%. Moreover, these assemblies appear relatively stiff and have diameters of around 8 - 9 nm.

Also, a less contrast central channel can be observed at several well resolved entities. As a result of their stiffness most of the aggregates were found densely adjoined. Cross-sectional circular views like those described for the aggregates of **2** (cp. above) could not be observed here because the rods are too long and too rigid to become orientated perpendicular to the thin (100 to 300 nm) ice films. Nevertheless, from the uniform thickness of the aggregates a circular profile can be assumed. This assumption became quite more evident when the sample was prepared in an aqueous mixture with 10% (v/v) of methanol (see SI).

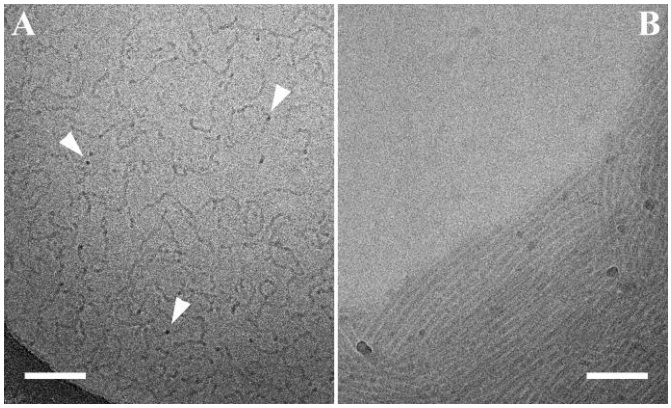

Figure 5. Cryo-TEM micrographs of amphiphiles **2** and **3** which both form fibrous aggregates in water. According to the hydrophobic length of the constituting compounds they strongly differ in diameter and flexibility. Twinned amphiphile **2** forms flexible micellar threads with 5 nm in diameter (A) of which frequently cross sectional top views can be recognized as dark spots along the threads course (white arrowheads), while its homologue **3** assembles into thicker (~8.5 nm) and more rigid rods (B). Bars represent 100 nm.

Herein, the number of aggregates was reduced due to the enhanced solubility and individual rods with diameters of about 9 nm were visible. However, groups of parallel rods were frequently found giving the opportunity to compare the rod morphology from both solvents in detail. Obviously, minor changes of the solvents' polarity do not significantly affect the overall architecture of the emerging aggregates and thus justifies the use of solvent mixtures slightly differing in polarity, e.g. for amphiphile **1**.

Micrographs of vitrified samples of the best water-soluble amphiphile **4** (0.5% wt in pure water) displayed two different kinds of assembly structures (**Figure 6A**), i.e. (i) spherical entities with a relatively narrow sizes distribution of 14 to 18 nm (central region in Figure 6A) tending to form highly ordered arrays and (ii) markedly larger smooth unstructured structures of higher contrast with different diameters up to the micrometer scale (black-rimmed arrows). FFT of the densely packed arrays allowed for a precise determination of the aggregates dimensions. The sharp reflexes in the Fourier transform (inset in **Figure 6B**) assign ideally hexagonal arranged entities of very uniform repeat distances of 8.2 ± 0.3 nm. Given the size and the noticeable monodispersity, these aggregates have to be considered as globular micelles.

The micelle arrays feature sharp boundaries against the surrounding vitrified solvent giving the impression of attractive interactions between the micelles (white arrow heads in **Figure 6A**). To further investigate the extent of assembly interactions, cryo-TEM measurements of a diluted sample of **4** at 0.25% (wt) in water were performed. Hereby, individually distributed globular micelles but none of the larger aggregates were observed (**Figure 6C**), providing strong evidence that the hexagonal arrays originate rather from a dense arrangement due to high local concentration of assemblies than from assembly interactions.

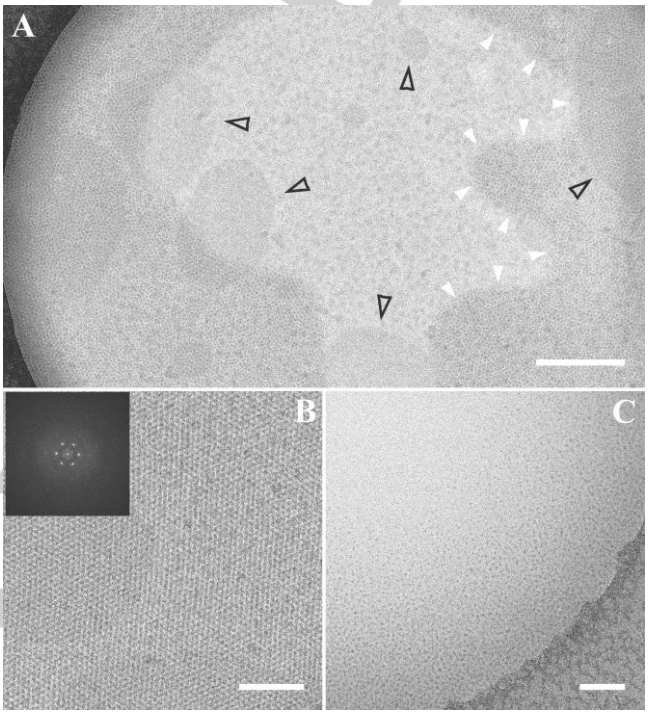

Figure 6. *Cryo-TEM* images of the 0.5 wt% aqueous solution of **4** exhibit spherical micelles of 14 to 18 nm (central region) next to featureless large aggregates of different diameters (black-rimmed arrowheads) (A) Arrays of densely packed micelles which sometimes present an ideally hexagonal arrangement (B) display sharp peaks in the Fourier transform (inset), which correspond to 8.2 ± 0.3 nm distances in real space. Dissolution of the sample to 0.25 wt% gives individual micelles (C).
Bars represent 200 nm (A) or 100 nm (B and C).

The microscopic data proof a marked relationship between molecular and supramolecular structure for the reported series of compounds. The increase of curvature starting with two-dimensional ribbons (**1**) via one-dimensional fibers and rods (**2** and **3**, respectively) into globular micelles (**4**) is in line with the concept of a hydrophilic-hydrophobic balance defining the assembly curvature according to Israelachvili *et al.*[40,41] i.e. amphiphile **1** with long hydrophobic tails and short hydrophilic head groups forms rather planar aggregates with low curvature, whereas amphiphiles **2** and **3** with their "balanced" ratio of hydrophobic and hydrophilic constituents (short tails and heads or long tails and heads, respectively) are forming micellar fibres of moderate curvature (**Figure 7**, top and centre). Amphiphile **4** with short tails and large head groups assembles into small spherical aggregates of highest curvature (**Figure 7**, bottom).

Thus, it can be stated that the classical concept of the interdependence of assembled architecture and packing parameter also holds for this group of compounds with their flexible twinned head groups and tails and their bi-aromatic spacer. Moreover, here the longer hydrophobic tails of **1** and **3** account not only for thicker and broader ribbons and rods but also for obviously more rigid assemblies, if compared to the flexible threads from amphiphile **2**.

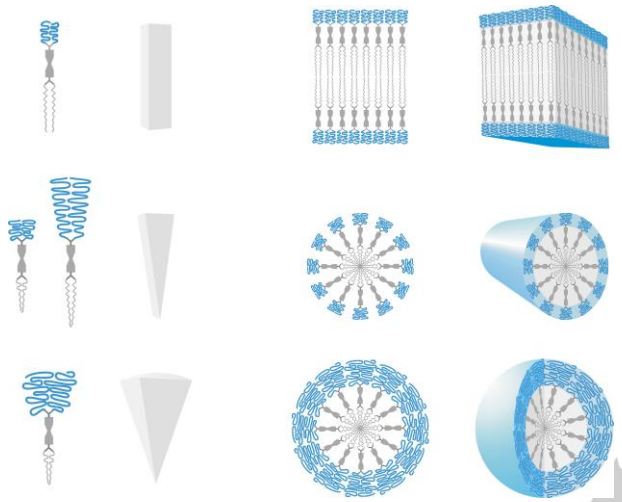

Figure 7. Aggregation behaviour of twinned amphiphiles **1**-**4**. Amphiphile **1** containing a comparatively large hydrophobic part and only short hydrophilic PEO chains resembles a cylindrical shape and hence forms ribbon-like aggregates, i.e. planar bilayers (top row). The long PEO chains and short alkyl moieties result in a prominently cone-shaped geometry in the case of **4** which assemble into highly curved globular micelles (bottom row). In the case of **2** and **3**, where head groups are only moderately larger than the hydrophobic tails, and slightly cone-shaped geometry drives the aggregation towards fibrous or rod-like nanostructures (middle row).

Table 1. Structural data of amphiphiles **1** – **4**.

Compound	Aggregate type	Visible thickness/diameter [nm]	Overall diameter * [nm]	Calculated invisible shell* [nm]
C_{18}/mPEG350 (**1**)	ribbons	8.5 ± 0.5	-	-
C_{11}/mPEG350 (**2**)	micellar threads	5.1 ± 0.4	-	-
C_{18}/mPEG1000 (**3**)	micellar rods	8.5 ± 0.5	13.8 ± 0.3	2.6 ± 0.4
C_{11}/mPEG1000 (**4**)	globular micelles	5.0 ± 1.0	8.2 ± 0.3	1.6 ± 0.5

** Diameters calculated from FFT of densely arranged aggregates which were found only in preparations of **3** and **4**.*

Table 1 clearly demonstrates coinciding dimensionalities of the aggregates with regard to the lengths of the amphiphiles. Thus, aggregates from both compounds containing the stearic acid tails (**1** and **3**) have a visible thickness/diameter of about 8.5 nm. Whereas the aggregates from undecenoic acid substituted amphiphiles (**2** and **4**) display diameters of about 5 nm. Modelling of the twinned amphiphiles provided evidence for the molecular construction of the observed aggregates. If a bilayer (**1**) or bimolecular (**3**) arrangement of the molecules is assumed, both the dimensions (*vide supra*) coincide fairly well with the length of the hydrophobic parts of the constituting twinned amphiphiles (i.e. the distance between the terminal hydrogen and the carboxylic oxygen of the head group binding ester group) which is 3.8 and 3.0 nm, respectively (**Figure 1**). Furthermore, the difference between these dimensions and the assemblies' distances extracted from FFT measurements on clustered aggregates from **3** and **4** (*vide supra*) indicates that their hydrophilic domain is not visible in TEM, which is a known phenomenon in the case of PEG head groups.[42] In the case of aggregates from **1** and **3** (C_{18}), the articulate electron density disparities between the bi-aromatic central spacer and the hydrocarbon tails generate a density profile (light centre and dark edges) for the hydrophobic region alone, which clearly suggest a bilayer (**1**) or bimolecular (**3**) arrangement, respectively.

Besides this straight forward construction model, there also remain some observations to be mentioned. The observed 8.5 nm bilayer thickness (**1**) or diameter of the rods (**3**) are both larger than expected from the molecular structure of the constituting amphiphiles, i.e. they are larger than double the molecules hydrophobic length (*vide supra*). On the other hand, visible diameters of the micellar threads and globular micelles from compounds **2** and **4**, respectively, are slightly smaller (5 instead of 6 nm) in this regard. Also note that, although amphiphiles **3** and **4** contain the same mPEG1000 head groups, the calculated hydrophilic shell thickness (**Table 1**) of the micelles from **4** (1.6 nm) is about 38% thinner than that of the micellar rods from **3** (2.6 nm). While both these short values clearly point to coiled arrangements of the PEG chains, beyond this, one can only speculate about the origin of the marked shell thickness difference. It might be caused by slightly differing packings - most probably due to the bi-aromatic spacers - of the short and long tailed twinned amphiphiles. The thinner hydrophilic shell hints to a more loose packing within the small micelles, which provides more lateral space for the PEG chains to coil resulting in a shorter radial extent. To the contrary, a dense packing of the hydrophobic cores forces the PEG chains to extend further and thus, effects a thicker hydrophilic shell. A tight assembly would also explain the slightly oversized visible thickness of the ribbons from **1** and the diameters of the rods

from **3**. Here, one may assume that the innermost parts of the PEG chains might contribute some contrast to the TEM micrographs due to a compacted arrangement next to the hydrophobic centres or that the core region is not exactly determined due to packing offsets like those that were shown earlier by Padia *et al.* for short PEO chain amphiphiles.[43] Likewise, the varying stiffness of the micellar threads (**2**) and the rods (**3**) hints to more compact packing within the latter. Nevertheless, since we lack a measure for the shell thickness of the aggregates from **1** and **2** this explanation remains partly hypothetic. Finally, although no direct evidence like a bilayer profile was found for the micellar threads and globular micelles from **2** and **4**, respectively, it seems to be reasonable to also assume a bimolecular construction with the PEG shell being invisible, again.

Cytotoxicity

To test the suitability of the amphiphiles **2**, **3**, and **4** for biological and clinical applications, a cytotoxicity study was performed by real time cell analysis (RTCA) using human A549 lung cancer cells (**Figure 8**). All amphiphiles were well tolerated up to a concentration of 0.1 mg ml^{-1} and even an extended incubation for up to 3 days did not result in an increased toxicity (**SI Figure 20**). Amphiphile **3** with the longest alkyl chain showed the best compatibility and was even non-toxic up to the highest test concentration of 1 mg ml^{-1} and hence is considered most suitable for later medicinal applications e.g. as nano carrier for drug encapsulation.

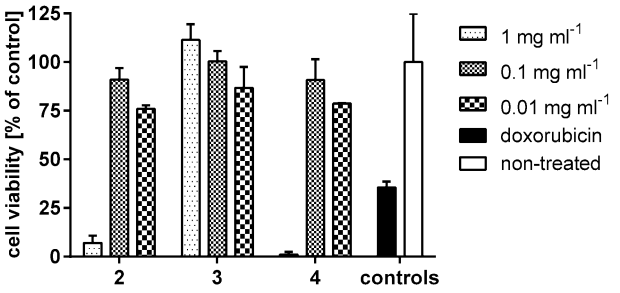

Figure 8: Cell viability test of amphiphiles **2**, **3**, and **4** by real time cell analysis (RTCA) of A549 adenocarcinomic human alveolar basal epithelial cells. End point data of cells treated for 24 hours was used to calculate the toxicity of the amphiphiles compared to non-treated control cells. The cytostatic drug doxorubicin (1 µM) was used as a positive control. Measurements were performed in triplicate and data represent the mean ± standard deviation (SD).

Guest encapsulation study

Our interest is to understand the influence of different structural constituents of these twinned amphiphiles on their encapsulation capacity. The potential of these amphiphiles as nanocarriers for hydrophobic guests was investigated using two hydrophobic guest molecules i.e. Nile Red and Nimodipine. Nile Red is a poorly water soluble, neutral and environmentally sensitive fluorescent dye. It exhibit highly solvatochromic fluorescence with strong emission in lipophilic environment.[44] Nile red encapsulation gives fair amount of information about the site of encapsulation in nano-architectures. While Nimodipine (NIM), a derivative of 1,4-dihydropyridine developed by Bayer AG in 1983, is a well-known calcium channel blocker. It is used to increase the cerebral blood flow in humans as well as in animals.[45] However, due to its poor aqueous solubility (0.4 mg/L^{-1}), the commercial formulation involves the use of polyethylene glycol (62.5 g) and ethanol (37.5 g) to solubilize 50 mg of Nimodipine.[34] Since our amphiphiles are constituted from PEG, they can enhance the solubility of Nimodipine besides facilitating its encapsulation and circulation in the biological systems.

The guest encapsulation experiments were carried out as reported in the literature.[46] A detailed description of the procedure as well as the mode of calculation of the encapsulation capacity is provided in the experimental section/ESI. Amphiphile **1** could not be considered for studying the transport potential due to its poor solubility in water. The transport capacity of different amphiphiles with identical mPEG and alkyl chains showed similar trends for the two different guest molecules, indicating a strong relation between transport capacity and structure of the hosting amphiphile. The transport capacity of Nile Red is found to be in line with our previous report on nonionic dendritic amphiphiles displaying unexpected parameters in micellar assemblies.[21] While for the Nimodipinie these systems found to be better than our previous reported system.[34,46,47] For amphiphiles **2** and **4** having short C_{11} alkyl chain, it was observed that increasing the length of the mPEG head group from Mn 350 (**2**) to 1000 (**4**) leads to considerably decreased transport capacity for either of the guest molecules. However, increasing the length of the alkyl chain from C_{11} to C_{18} like in case of amphiphile **3** led to an enhancement of the transport capacity (**Figure 9** and **Table 2**). Qualitative analysis of the data shows that the transport capacity depends on the length of both alkyl and mPEG chains, and hydrophilic-lipophilic balance of the amphiphile.

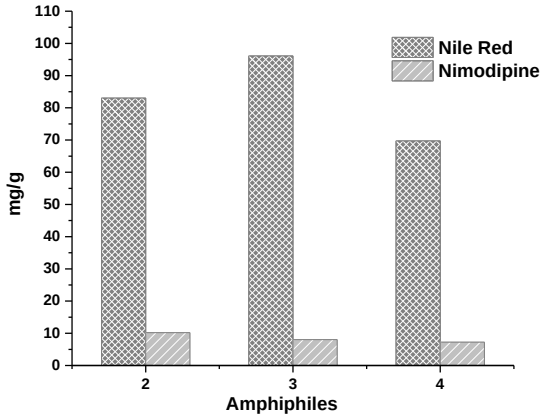

Figure 9. Evaluation of transport capacity of the amphiphiles **2**, **3**, and **4** using Nile red and Nimodipine.

Table 2. Calculation of transport capacity in mg/g [dye or drug (mg) /amphiphiles (g)].

Compound	Transport capacity (mg/g)	
	Nile Red	Nimodipine
C_{11}/mPEG350 (**2**)	10.18	83.04
C_{18}/mPEG1000 (**3**)	8.03	96.09
C_{11}/mPEG1000 (**4**)	7.23	69.74

Conclusions

A new series of non-ionic twinned amphiphiles with two hydrophilic mPEG head groups and two hydrophobic alkyl chains has been synthesized. The non-ionic PEG based amphiphiles have been readily prepared by utilizing 'Click chemistry' and acylation reactions on a chemo-enzymatically synthesized A_2B_2 monomer. The aggregation behaviour of these amphiphiles was investigated using fluorescence and DLS. Complementing on cryo-TEM measurements which proved the formation of globular, thread-like or rod-like micelles as well as planar double-layer assemblies, depending on the amphiphile's molecular structure. The observed morphologies are in line with the packing parameter model of Israelachvili. Homogeneous ordering of the aggregates from amphiphiles **3** and **4** at elevated concentrations provided the additional opportunity for determining the structural dimensions with high accuracy. The cytotoxicity study suggested the twinned amphiphiles **2**-**4** to be suitable for in vivo applications, their potential as nanocarriers was investigated using hydrophobic guest molecules Nile Red and Nimodipine showing that the Nile Red was more efficiently encapsulated by amphiphiles having lower HLB value if compared to Nimodipine. Additionally, a correlation between loading capacity and HLB of the amphiphiles emerged. The mPEG based twinned amphiphilic architecture introduced herein was found to be more efficient in means of drug loading capacity as compared to the dendritic amphiphilic architecture which was earlier reported by Thota *et al.*[46] The combined synthetic approach of simple and environmentally safe chemical steps along with the understanding of the aggregation behaviour observed for the synthesized amphiphiles opens up possibilities for design, synthesis and applications of new structural motifs based on twinned PEG amphiphiles.

Experimental Section

All the compounds were characterized by their physical and spectral data. Infrared spectra were recorded on a Perkin-Elmer FT-IR model 9 spectrophotometer. The ^{1}H and ^{13}C NMR spectra recorded on Jeol-400 (400 MHz, 100.5 MHz) NMR spectrometer using TMS as an internal standard. The chemical shift values are measured on δ scale and the coupling constant values (*J*) are reported in Hz. The HRMS data were recorded on Agilent-6530, Q-TOF LCMS.

All of the chemicals and solvents used were purchased from the Spectrochem Pvt. Ltd., SD Fine Chemicals Pvt. Ltd., Sigma-Aldrich, and Alfa Aesar. All the solvents were distilled prior to their use. Novozym 435 (immobilized *Candida antarctica* lipase) was purchased from Julich Chiral Solutions GmbH (Jülich, Germany). Reactions were monitored by pre-coated TLC plates (Merck silica gel 60 F254), by visualizing the spot in ceric solution stain and iodine. All the compounds were purified by column chromatography using silica gel (100-200 mesh).

Procedure for the synthesis of 2-azidopropane-1,3-diol

1,3-Diacetoxyglycerol and 2-azidopropane-1,3-diol were synthesized according to the published procedures and spectral data obtained were found to be identical with those reported in the literature.[36]

2-Azidopropane-1,3-diyl distearate (5)

2-Azidopropane-1,3-diol (1 g, 8.54 mmol) and stearic acid (7.29 g, 25.64 mmol) were dissolved in DCM (30 mL). The solution was maintained at 0 °C, then EDC.HCl (4.89 g, 25.64 mmol) and DMAP (1.25 g, 10.25 mmol) were added. The reaction mixture was allowed to warm up to room temperature and stirred at 30 °C for 15 h. Progress of the reaction was monitored by TLC using ethyl actate/petroleum ether (1:9) (R_f = 0.6). On completion of the reaction, the reaction mixture was concentrated under reduced pressure and the obtained crude was suspended in water and ethyl acetate (3 x 30 mL). The

combined organic layers were dried over anhydrous Na_2SO_4 and the solvent evaporated to yield the crude product, which was purified through column chromatography using ethyl acetate/petroleum ether to give the desired compound **5** in 93% yield. ^{1}H NMR (400 MHz, $CDCl_3$): δ = 4.31-4.11 (m, 4H, -OCH(**CH₂**O-)$_2$), 3.47-3.45 (m, 1H, -N_3**CH**(CH_2O-)$_2$), 2.37-2.29 (m, 4H, -OOC**CH₂**CH_2-), 1.67-1.59 (m, 4H, -OOCCH_2**CH₂**-), 1.29-1.20 (m, 56H, **Alkyl chain**), 0.88 ppm (t, *J* = 4.0 Hz, 6H, -**CH₃**). ^{13}C NMR (100.5 MHz, $CDCl_3$): δ = 173.41, 63.15, 58.83, 34.15, 32.07, 29.83, 29.59, 29.38, 29.24, 24.95, 22.83, 14.25. HRMS: *m/z* [M+Na^+] calcd for $C_{39}H_{75}NaN_3O_4$: 649.5758; found: 672.5660. IR(KBr) ν_{max} 2916, 2849, 2130, 1743, 1467 cm^{-1}.

2-azidopropane-1,3-diyl bis(undec-10-enoate) (6)

2-Azidopropane-1,3-diol (1 g, 8.54 mmol) and undecylenic acid (7.29 g, 25.64 mmol) were dissolved in DCM (30 mL). The solution was kept on ice to maintain the temperature at 0 °C, then EDC.HCl (1.25 g, 10.25 mmol) and DMAP (4.89 g, 25.6 mmol) were added. The reaction mixture was allowed to warm up to room temperature and stirred at 30 °C for 15 h. Progress of the reaction was monitored by TLC using ethyl actate/petroleum ether (1:9) (R_f = 0.6). Upon completion of the reaction, the reaction mixture was concentrated under reduced pressure and obtained product was extracted with ethyl acetate (3 x 30 mL) and water. The combined organic layers were dried over anhydrous Na_2SO_4 and the solvent evaporated to yield the crude product, which was then purified through column chromatography using ethyl acetate/petroleum ether to give the desired compound **6** in 93% yield. ^{1}H NMR (400 MHz, $CDCl_3$): δ = 5.84-5.74 (m, 2H, CH_2=**CH**-), 5.00-4.90 (m, 4H, **CH₂**=CH-), 4.24-4.10 (m, 4H, -O**CH**(CH_2O-)$_2$), 3.89-3.83 (m, 1H, -N_3**CH**(CH_2O-)$_2$), 2.36-2.29 (m, 4H, -OOC**CH₂**CH_2-), 2.05-2.00 (m, 4H, CH_2=CH-**CH₂**-), 1.64-1.60 (m, 4H, -OOCCH_2**CH₂**-), 1.40-1.25 (m, 20H, alkyl chain). ^{13}C NMR (100.5 MHz, $CDCl_3$): δ = 173.33, 139.24, 114.26, 63.11, 58.79, 34.09, 33.87, 29.36, 29.20, 29.16, 29.13, 28.98, 24.89. HRMS: *m/z* [M+Na^+] calcd for $C_{25}H_{43}NaN_3O_4$: 449.3254; found: 472.3174. IR (Film) ν_{max} = 2952, 2854, 2125, 1740, 1462 cm^{-1}.

mPEG-350 acid (7)

Mono-methoxy poly(ethylene glycol) (M_w: 350) (5 g, 10 mmol) was dissolved in distilled water (50 mL) in a 250 mL round-bottom flask and (2.2 g, 40 mmol) of sodium hydroxide was added. The reaction mixture was stirred in ice bath to allow the temperature to reach 0 °C, then 13.5 g, 60 mmol of potassium permanganate was added in small amounts for approx. 2 to 3 hr. The reaction mixture was allowed to warm at room temperature and left for stirring at 80 °C for 24 h. Progress of the reaction was monitored by TLC. On completion of the reaction, the black residue was filtered off. The filtrate was acidified using 2 M hydrochloric acid solution to pH 2 and then extracted with chloroform (4 x 50 mL). The organic layers was dried over anhydrous sodium sulfate, and concentrated under reduced pressure to get the desired mPEG acid, **7** in 91% yield; ^{1}H NMR (400 MHz, $CDCl_3$): δ = 4.12 (s, 2H, HOOC**CH₂**O-mPEG), 3.71-3.50 (m, 24H, **mPEG** region), 3.34 (s, 3H, **CH₃**O-mPEG). ^{13}C NMR (100.5MHz, $CDCl_3$): δ = 172.21, 71.80, 71.66, 70.33, 68.89 58.93. IR(neat) ν_{max} = 2868, 1741, 1455 cm^{-1}.

mPEG-1000 acid (8)

Mono-methoxy poly(ethylene glycol) (M_w: 1000) (5 g, 10 mmol) was dissolved in distilled water (50 mL) in a 250 mL round-bottom flask and 0.8 g, 40 mmol of sodium hydroxide was added The reaction mixture was stirred in ice bath to allow the temperature to reach 0 °C, then (4.7 g, 60 mmol) of potassium permanganate was added in small amounts for approx. 1-2 hr. The reaction mixture was allowed to warm at room temperature and then heated to 80 °C for 24 h. Progress of the reaction was monitored by TLC. On completion of the reaction, black residue was filtered off. The filtrate was acidified using 2 M hydrochloric acid solution to pH 2 and then extracted with chloroform (6 x 50 mL). The organic layers was dried over anhydrous sodium sulfate, and concentrated under reduced pressure to get the desired mPEG acid, **8** in 91% yield. ^{1}H NMR (400 MHz, $CDCl_3$): δ = 4.10 (s, 2H, HOOC**CH₂**O-mPEG), 3.70-3.53 (m, 83H, **mPEG** region), 3.37 (s, 3H, **CH₃**O-mPEG). ^{13}C NMR (100.5 MHz, $CDCl_3$): δ = 172.0, 71.88, 70.95, 70.51, 68.80, 58.98. IR (Film) ν_{max} = 2865, 1743, 1465 cm^{-1}.

2-(4-(ethoxycarbonyl)phenoxy)propane-1,3-diyl diacetate (9)

To a stirring solution of ethyl 4-hydroxybenzoate (1 g, 6.02 mmol), 1, 3-diacetoxyglycerol (1.5 g, 9.02 mmol) and triphenylphosphine (3.15 g, 12.03 mmol) in toluene (20 mL), diethyl azodicarboxylate in 5 mL of toluene was added drop wise The reaction mixture was stirred for 15 h at 30 °C. The progress of the reaction was monitored by TLC using ethyl acetate/petroleum ether (3:7) (R_f = 0.4). On completion of the reaction, toluene was removed under reduced pressure and the crude was suspended in water and ethyl acetate (3 x 30 mL). The combined organic layers were dried over Na_2SO_4 and the solvent evaporated to yield the crude product, which was purified through column chromatography using petroleum

ether/ethyl acetate to give the desired compound **9** as a viscous liquid in 83% yield. ^{1}H NMR (400 MHz, $CDCl_3$): δ = 7.99 (d, *J* = 8.0 Hz, 2H, aromatic **CH**), 6.99 (d, *J* = 8.0 Hz, 2H, aromatic **CH**), 4.79-4.75 (m, 1H, -O**CH**(CH_2O-)$_2$), 4.37-4.26 (m, 6H, -OCH(**CH_2**O-)$_2$) and -O**CH_2**CH_3), 2.06 (s, 6H, **-**CO**CH_3**), 1.37 (t, *J* = 8.0 Hz, 3H, -CH_2**CH_3**). ^{13}C NMR (100.5 MHz, $CDCl_3$): δ = 170.79, 166.29, 161.41, 131.81, 124.15, 115.45, 73.57, 62.75, 60.91, 20.87, 14.50. HRMS (positive, MeOH): *m/z* [M+Na^+]: calcd for $C_{16}H_{20}NaO_7$: 324.1209; found: 347.1089. IR(film) v_{max} = 3743, 2981, 1743, 1710, 1605, 1510 cm^{-1}.

4-((1,3-dihydroxypropan-2-yl)oxy)benzoic acid (10)

Compound **9** (6 g, 15.43 mmol) was dissolved in a methanolic solution of NaOH (1N) (30 mL) and water (10 mL), the reaction mixture was stirred at 50 °C for 4 h. Progress of the reaction was monitored by TLC using methanol/chloroform (1:9) (R_f = 0.15). Upon the completion of the reaction, reaction mixture was neutralized with dil. HCl and concentrated under reduced pressure to obtain the crude product which was purified through column chromatography using chloroform/methanol to give the desired compound **10** in 95% yield. ^{1}H NMR (400 MHz, CD_3OD): 7.97 (d, *J* = 8.0 Hz, 2H, aromatic **CH**), 7.08 (d, *J* = 8.0 Hz, 2H, aromatic **CH**), 4.87-4.49 (m, 1H, -O**CH**(CH_2OH)$_2$), 3.81-3.78 (m, 4H, -OCH(**CH_2**OH)$_2$). ^{13}C NMR (100.5 MHz, CD_3OD): δ = 169.90, 164.02, 132.81, 124.18, 116.60, 80.43, 61.87. HRMS: *m/z* [M+Na^+] calcd for $C_{10}H_{12}NaO_5$: 212.0685; found: 235.0586. IR(neat) v_{max} = 3736, 3615, 2925, 2853, 2312, 1740, 1514 cm^{-1}.

Prop-2-yn-1-yl 4-((1,3-dihydroxypropan-2-yl)oxy)benzoate (11)

To a solution of compound **10** (3.5 g, 16.50 mmol) in DMF (40 mL), potassium carbonate (4.5 g, 33 mmol) was added, the reaction mixture was stirred for 15 min at 60 °C. To this reaction mixture, propargyl bromide was slowly added (2.35 g, 19.80 mmol). This reaction mixture stirred at 60 °C for 6 h. Progress of the reaction was monitored by TLC using chloroform/methanol (9:1) (R_f = 0.3). On completion of the reaction, reaction mixture was concentrated under reduced pressure and the obtained crude product was suspended in water and ethyl acetate (3 x 25 mL). The combined organic layers were dried over Na_2SO_4 and the solvent evaporated to yield the crude product, which was purified through column chromatography using chloroform /methanol to give the desired compound **11** in 87% yield. ^{1}H NMR (400 MHz, $CDCl_3$): δ = 7.98 (d, *J* = 8.0 Hz, 2H, aromatic **CH**), 6.98 (d, *J* = 8.0 Hz, 2H, aromatic **CH**), 4.86 (d, *J* = 2.3 Hz, 2H, -**CH_2**C≡CH), 4.54-4.49 (m, 1H, -O**CH**(CH_2OH)$_2$), 3.94-3.86 (m, 4H, -OCH(**CH_2**OH)$_2$), 2.50 (t, *J* = 2.3 Hz, 1H, -CH_2C≡**CH**). ^{13}C NMR (100.5 MHz, $CDCl_3$) : δ = 165.51, 161.99, 132.19, 122.62, 115.51, 78.33, 77.98, 75.06, 62.05, 52.44. HRMS : *m/z* [M+Na^+] calcd for $C_{13}H_{14}NaO_5$: 212.0685; found: 235.0586. IR(neat) v_{max} = 3291, 2309, 1713, 1604, 1508 cm^{-1}.

Synthesis of compound 12

Compound **11** (0.5 g, 2 mmol) and 2-azidopropane-1,3-diyl distearate (**5**, 1.56 g, 2.4 mmol) were dissolved in 20 mL THF/water (3:1) followed by the addition of copper sulfate (0.199 g, 0.8 mmol) and sodium ascorbate (0.079 g, 0.4 mmol). The reaction mixture was then stirred at 50 °C for 15 h. Progress of the reaction was monitored by TLC using chloroform/ methanol (9:1) (R_f = 0.55). On completion of the reaction, the reaction mixture was concentrated under reduced pressure and the obtained crude product was suspended in chloroform (3 x 20 mL) and water. The combined organic layers were dried over anhydrous Na_2SO_4 and the solvent evaporated to yield the crude product which was subsequently purified through column chromatography using chloroform/methanol to give the desired compound **12** in 93% yield. ^{1}H NMR (400 MHz, $CDCl_3$): δ = 7.95 (d, *J* = 8.0 Hz, 2H, aromatic **CH**), 7.78 (s, 1H, triazolyl ring **CH**), 6.95 (d, *J* = 8.0 Hz, 2H, aromatic **CH**), 5.42 (s, 2H, -O**CH_2**-triazole), 5.10-5.04 (m, 1H, triazole-**CH**(CH_2O-)$_2$), 4.52-4.48 (m, 5H, -O**CH**(CH_2OH)$_2$ and triazole-CH(**CH_2**O-)$_2$), 3.95-3.86 (m, 4H, -OCH(**CH_2**OH)$_2$), 2.34-2.24 (m, 2H, -OOC**CH_2**CH_2-), 1.58-1.51 (m, 4H, -OOCCH_2**CH_2**-), 1.28-1.23 (m, 56H, alkyl chain), 0.87 (t, *J* = 4.0 Hz, 6H, -**CH_3**)). ^{13}C NMR (100.5 MHz,$CDCl_3$): δ **=** 172.83 165.82, 161.66, 142.95, 131.76, 123.62, 122.54, 115.16, 78.09, 62.04, 61.70, 58.49, 57.52, 33.67, 31.73, 29.51, 29.46, 29.41, 29.25, 29.16, 29.01, 28.84, 24.51, 22.49, 13.92. HRMS: *m/z* [M+Na^+] calcd for $C_{52}H_{89}NaN_3O_9$: 899.6599; found: 922.6496. IR (Film) v_{max} = 3743, 2914, 2855, 1738, 1463 cm^{-1}.

Synthesis of compound 13

Compound **11** (0.5 g, 2 mmol) and 2-azidopropane-1,3-diyl bis(undec-10-enoate) (**6**, 1.08 g, 2.4 mmol) were dissolved in 20 mL THF/water (3:1) followed by the addition of copper sulfate (0.199 g, 0.8 mmol) and sodium ascorbate (0.079 g, 0.4 mmol). The reaction mixture was then stirred at 50 °C for 15 h. Progress of the reaction was monitored by TLC using chloroform/ methanol (9:1) (R_f = 0.55). On completion of the reaction, the reaction mixture was concentrated under reduced pressure and the obtained crude product was suspended in water and chloroform (3 x 20 mL). The combined organic layers were dried over anhydrous Na_2SO_4. The solvent evaporated to yield the

crude product, which was subsequently purified through column chromatography using chloroform/methanol to give the desired compound **13** in 93% yield. ^{1}H NMR (400 MHz, $CDCl_3$): δ = 7.96 (d, *J* = 8.0 Hz, 2H, aromatic **CH**), 7.78 (s, 1H, triazolyl ring **CH**), 6.96 (d, *J* = 8.0 Hz, 2H, aromatic **CH**), 5.84-5.74 (m, 2H, CH_2=**CH**-), 5.43 (s, 2H, -O**CH₂**-triazole), 5.11-5.05 (m, 1H, triazole-**CH**(CH_2O-)$_2$), 5.00-4.90 (m, 4H, **CH₂**=CH-), 4.55-4.46 (m. 5H, -O**CH**(CH_2OH)$_2$) and triazole-CH(**CH₂**O-)$_2$), 3.96-3.88 (m, 4H, -OCH(**CH₂**OH)$_2$), 2.28-2.24 (m, 4H, -OOC**CH₂**CH_2-), 2.04-1.99 (m, 4H, CH_2=CH-**CH₂**-), 1.62-1.52 (m, 4H, -OOCCH_2**CH₂**-), 1.37-1.18(m, 20 H, alkyl chain). ^{13}C NMR (100.5 MHz, $CDCl_3$): δ = 172.79, 165.76, 161.67, 142.93, 138.94, 131.73, 123.61, 122.47, 115.14, 113.97, 62.03, 61.66, 58.49, 57.50, 33.64, 29.03, 28.98, 28.82, 28.65, 24.47. HRMS: *m/z* [M+Na$^+$] calcd for $C_{38}H_{57}NaN_3O_9$: 699.4095; found: 722.4019. IR (neat) ν_{max} = 2923, 2864, 1742, 1604, 1508 cm^{-1}.

Synthesis of compound 1

Compound **12** (0.5 g, 0.55 mmol) and mPEG 350 acid (**7**, 0.583 g, 1.66 mmol) were dissolved in DCM (30 mL). The mixture was stirred under ice cold conditions to maintain the temperature at 0ºC. Then EDC.HCl (0.318 g, 1.66 mmol) and DMAP (0.081 g, 0.66 mmol) were added. The reaction mixture was allowed to warm up to room temperature and left for stirring at 30 ºC for 15 h. Progress of the reaction was monitored by TLC using chloroform/methanol (9:1) (R_f = 0.4). On completion of the reaction, the reaction mixture was concentrated under reduced pressure and the obtained crude was suspended in water and chloroform (3 x 20 mL). The combined organic layers were dried over anhydrous Na_2SO_4 and the solvent evaporated to yield the crude product which was further purified through column chromatography using chloroform/methanol to give the desired compound **1** in 91% yield. ^{1}H NMR (400 MHz, $CDCl_3$): δ = 7.99 (d, *J* = 8.0 Hz, 2H, aromatic **CH**), 7.77 (s, 1H, triazolyl ring **CH**), 6.98 (d, *J* = 8.0 Hz, 2H, aromatic **CH**), 5.44 (s, 2H, -O**CH₂**-triazole), 5.09-5.06 (m, 1H, triazole-**CH**(CH_2O-)$_2$), 4.80-4.78 (m, 1H, -O**CH**(CH_2O-)$_2$), 4.55-4.49 (m, 4H, triazole-CH(**CH₂**O-)$_2$), 4.43-4.34 (m, 4H, -CH(**CH₂**O-)$_2$), 4.16 (s, 4H, -OOC**CH₂**O-mPEG), 3.75-3.54 (m, 44H, **mPEG** region), 3.37 (s, 6H, **CH₃**O-PEG), 2.28 (t, *J* = 4.0 Hz, 4H, -OOC**CH₂**CH_2-), 1.54-1.56 (m, 4H, -OOCCH_2**CH₂**-) 1.30-1.24 (m, 56H, alkyl chain), 0.87 (t, *J* = 4.0 Hz, 6H, -**CH₃**). ^{13}C NMR (100.5 MHz, $CDCl_3$): δ = 173.11, 170.27, 165.96, 161.46, 143.23, 132.17, 123.90, 123.46, 115.46, 72.08, 71.16, 70.73, 68.51, 62.64, 62.39, 59.17, 58.81, 57.95, 34.02, 32.06, 29.84, 29.80, 29.74, 29.49, 29.35, 29.18, 24.86, 22.83, 14.26. GPC: Mw = 1979, Mn = 1918, PDI = 1.032; IR (neat) ν_{max} = 2915, 2851, 1735, 1605, 1508 cm^{-1}.

Synthesis of compound 2

Compound **13** (**7**, 0.5 g, 0.71 mmol) and mPeg 350 acid (0.751 g, 2.14 mmol) were dissolved in DCM (30 mL). The reaction mixture was stirred under ice cold conditions to maintain the temperature at 0 ºC, then EDC.HCl (0.318 g, 1.66 mmol) and DMAP (0.081 g, 0.66 mmol) were added. The reaction mixture was allowed to warm at room temperature and left stirring at 30 ºC for 15 h. Progress of the reaction was monitored by TLC using chloroform/methanol (9:1) (R_f = 0.4). Upon completion of the reaction, reaction mixture was concentrated under reduced pressure and obtained crude product was suspended in water and chloroform (3 x 30 mL). The combined organic layers were dried over anhydrous Na_2SO_4 and the solvent evaporated to yield the crude product which was purified through column chromatography using chloroform/methanol to yield the desired compound **2** in 91% yield. ^{1}H NMR (400 MHz, $CDCl_3$): δ = 7.98 (d, *J* = 8.0, 2H, aromatic **CH**), 7.77 (s, 1H, triazolyl ring **CH**), 6.97 (d, *J* = 8.0 Hz, 2H, aromatic **CH**), 5.82-5.76 (m, 2H, CH_2=**CH**-), 5.44 (s, 2H, -O**CH₂**-triazole), 5.08-5.06 (m, 1H, triazole-**CH**(CH_2O-)$_2$), 4.99-4.90 (m, 4H, **CH₂**=CH-), 4.80-4.77 (m, 1H, -**CH**(CH_2O-)$_2$), 4.54-4.49 (m, 4H, triazole-CH(**CH₂**O-)$_2$), 4.43-4.34 (m, 4H, -CH(**CH₂**O-)$_2$), 4.15 (s, 4H, -OOC**CH₂**O-mPEG), 3.73-3.53 (m, 60H, **mPEG** region), 3.37 (s, 6H, **CH₃**O-mPEG), 2.27 (t, *J* = 4.0 Hz, 4H, -OOC**CH₂**CH_2-), 2.03-2.00 (m, 4H, CH_2=CH-**CH₂**-), 1.55-153 (m, 4H, -OOCCH_2**CH₂**-), 1.37-1.33 (m, 4H, -**CH₂**-), 1.29-1.25 (m, 16H, alkyl chain). ^{13}C NMR (100.5 MHz, $CDCl_3$): δ = 172.95, 170.89, 170.12, 165.81, 161.32, 139.12, 132.01, 123.75, 123.32, 115.31, 114.18, 73.12, 71.93, 70.67, 68.35, 62.47, 62.25, 59.02, 58.66, 57.82, 33.86, 33.75, 29.23, 29.02, 28.98, 28.85, 24.67 ppm; GPC: Mw = 1513, Mn = 1462, PDI = 1.034. IR (Film) ν_{max} = 2962, 2883, 1744, 1605, 1508, 1454 cm^{-1}.

Synthesis of compound 3

Compound **12** (0.5 g, 0.55 mmol) and mPEG 1000 acid (1.66 g, 1.66 mmol) were dissolved in DCM (30 mL). The reaction mixture was stirred under ice cold conditions to maintain the temperature at 0 ºC, then EDC.HCl (0.409 g, 2.14 mmol) and DMAP (0.104 g, 0.85 mmol) were added. After that, the reaction mixture was allow to warm at room temperature and left for stirring at 30 ºC for 15 h. Progress of the reaction was monitored by TLC using chloroform/methanol (9:1) (R_f = 0.4). Upon completion of the reaction, the reaction mixture was

concentrated under reduced pressure and the obtained crude was suspended in water and chloroform (3 x 20 mL). The combined organic layers were dried over anhydrous Na_2SO_4 and the solvent evaporated to yield the crude product which was purified through column chromatography using chloroform/methanol to give the desired compound **3** in 91% yield. ^{1}H NMR (400 MHz, $CDCl_3$): δ 7.97 (d, *J* = 8.0 Hz, 2H, aromatic **CH**), 7.77 (s, 1H, triazolyl ring **CH**), 6.98 (d, *J* = 8.0 Hz, 2H, aromatic **CH**), 5.44 (s, 2H, -O**CH₂**-triazole), 5.09-5.06 (m, 1H, triazole-**CH**(CH_2O-)$_2$), 4.80-4.77 (m, 1H, -**CH**(CH_2O-)$_2$), 4.54-4.47 (m, 4H, triazole-CH(**CH₂**O-)$_2$), 4.43-4.29 (m, 4H, -CH(**CH₂**O-)$_2$), 4.17-4.15 (m, 4H, -OOC**CH₂**O-mPEG), 3.74-3.53 (m, 190H, **mPEG** region), 3.37 (s, 6H, **CH₃**O-mPEG), 2.27 (t, *J* = 4.0 Hz, 4H, -OOC**CH₂**CH_2-), 1.56-1.53 (m, 4H, -OOCCH_2**CH₂**-), 1.29-1.24 (m, 56H, alkyl chain), 0.87 (t, *J* = 4.0 Hz, 6H, -**CH₃**). ^{13}C NMR (100 MHz, $CDCl_3$): δ = 172.92, 172.06, 165.76, 161.25, 132.03, 124.02, 123.97, 115.47, 109.96, 73.08, 71.89, 70.52, 68.29, 62.42, 62.13, 58.98, 58.61, 57.74, 33.83, 31.87, 29.65, 29.60, 29.55, 29.39, 29.16, 28.99, 24.65, 22.65, 14.04. GPC: Mw = 2555, Mn = 2154, PDI = 1.186. IR (Film) ν_{max} = 3014, 2924, 1746, 1462 cm^{-1}.

Synthesis of compound 4

Compound **13** (0.5 g, 0.71 mmol) and mPEG 1000 acid (2.14 g, 2.14 mmol) were dissolved in DCM (30 mL). The reaction mixture was stirred on ice to maintain the temperature at 0 ^{o}C, then EDC.HCl (0.409 g, 2.14 mmol) and DMAP (0.104 g, 0.85 mmol) were added. Afterwards the reaction mixture was allowed to warm up to room temperature and was left for stirring at 30 ^{o}C for 15 h. Progress of the reaction was monitored by TLC using chloroform/methanol (9:1) (R_f = 0.4). On completion of reaction, reaction mixture was concentrated under reduced pressure and obtained crude was suspended in water and chloroform (3 x 20 mL). The combined organic layers were dried over anhydrous Na_2SO_4 and the solvent evaporated to yield the crude product which purified through column chromatography using chloroform/methanol to give the desired compound **4** in 91% yileld. ^{1}H NMR (400 MHz, $CDCl_3$): δ = 7.93 (d, *J* = 8.0 Hz, 2H, aromatic **CH**), 7.72 (s, 1H, triazolyl ring **CH**), 6.93 (d, *J* = 8.0 Hz, 2H, aromatic **CH**), 5.78-5.68 (m, 2H, -CH_2=**CH**-), 5.38 (s, 2H, -O**CH₂**-triazole), 5.05-5.01 (m, 1H, triazole-**CH**(CH_2O-)$_2$), 4.99-4.80 (m, 4H, -**CH₂**=CH-), 4.75-4.71 (m, 1H, -**CH**(CH_2O-)$_2$), 4.51-4.43 (m, 4H, triazole-CH(**CH₂**O-)$_2$), 4.40-4.28 (m, 4H, -CH(**CH₂**O-)$_2$), 4.19 (s, 4H, - OOC**CH₂**O-mPEG), 3.77-3.39 (m, 182 H, **mPEG** region), 3.30 (s, 6H, **CH₃**O-mPEG), 2.21 (t, *J* = 4.0 Hz, 4H, -OOC**CH₂**CH_2-)1.99-1.96 (m, 4H, -CH_2=CH-**CH₂**-), 1.50-1.47 (m, 4H, -OOCCH_2**CH₂**-), 1.34-1.19 (m, 20H, alkyl chain). ^{13}C NMR (100.5 MHz, $CDCl_3$): δ = 173.09, 170.23, 166.15, 161.25, 143.19, 139.25, 132.12, 123.89, 115.38, 114.30, 72.02, 70.64, 70.64, 68.40, 62.55, 62.34, 59.14, 58.73, 33.96, 33.87, 29.34, 29.23, 29.13, 29.08, 28.95, 24.78. GPC: Mw = 2339, Mn = 1967, PDI = 1.189, IR (neat) ν_{max} = 2914, 2855, 1737, 1606, 1463 cm^{-1}.

Acknowledgements

We gratefully acknowledge the financial support from German Science Foundation (DFG) and SERB-DST, Government of India, and University of Delhi.

Keywords: Twinned amphiphiles • Self-assembly• *cryo*-TEM • nanocarriers • Nile Red, Nimodipine

[1] K. Baek, I. Hwang, I. Roy, D. Shetty, K. Kim, *Acc. Chem. Res.* **2015**, *48*, 2221-2229.

[2] E. Busseron, Y. Ruff, E. Moulin, N. Giuseppone, *Nanoscale* **2013**, *5*, 7098-7140.

[3] G. M. Whitesides, M. Boncheva, *PNAS* **2002**, *99*, 4769-4774.

[4] B. N. S. Thota, L. H. Urner, R. Haag, *Chem. Rev.* **2016**, *116*, 2079-2102.

[5] G. M. Whitesides, B. Grzybowski, *Science* **2002**, *295*, 2418-2421.

[6] C. Wang, Z. Wang, X. Zhang, *Small* **2011**, *7*, 1379-1383.

[7] C. Wang, Z. Wang, X. Zhang, *Acc. Chem. Res.* **2012**, *45*, 608-618.

[8] A. Sorrenti, O. Illa, R. M. Ortuño, *Chem. Soc. Rev.* **2013**, *42*, 8200-8219.

[9] T. Shimizu, M. Masuda, H. Minamikawa, *Chem. Rev*. **2005**, *105*, 1401-1443.

[10] L. C. Palmer, S. I. Stupp, *Acc. Chem. Res.* **2008**, *41*, 1674-1684.

[11] P. Huang, D. Wang, Y. Su, W. Huang, Y. Zhou, D. Cui, X. Zhu, D. Yan, *J. Am. Chem. Soc.* **2014**, *136*, 11748-11756.

[12] R. Zana, J. Xia, Marcel Dekker. New York. Chapter 1 (2003).

[13] R. Zana, *J. Colloid Interface Sci*. **2002**, *248*, 203-220.

[14] Y. Han, Y. Wang, *Phys. Chem. Chem. Phys.* **2011**, *13*, 1939-1956.

[15] F. M. Menger, J. S. Keiper, *Angew. Chem. Int. Ed.* **2000**, *39*, 1906-1920.

[16] S. K. Hait, S. P. Moulik, *Curr. Sci*. **2002**, *82*, 1101-1111.

[17] A. M. Cardoso, C. M. Morais, A. R. Cruz, A. L. Cardoso, S. G. Silva, M. L. do Vale, E. F. Marques, M. C. de Lima, A. S. Jurado, *Mol. Pharm.* **2015**, *12*, 716-730.

[18] A. M. Cardoso, C. M. Morais, A. R. Cruz, S. G. Silva, M. L. do Vale, E. F. Marques, M. C. P. de Lima, A. S. Jurado, *Eur. J. of Pharm. Biopharm*. **2015**, *89*, 347-356.

[19] S. Bhattacharya, A. Bajaj, *Chem. Commun*. **2009**, 4632-4656.

[20] H. Lv, S. Zhang, B. Wang, S. Cui, J. Yan, *J. Control. Release* **2006**, *114*, 100-109.

[21] B. Trappmann, K. Ludwig, M. R. Radowski, A. Shukla, A. Mohr, H. Rehage, C. Böttcher, R. Haag, *J. Am. Chem. Soc*. **2010**, *132*, 11119-11124.

[22] R. S. G. Krishnan, S. Thennarasu, A. B. Mandal, *J. Phys. Chem. B* **2004**, *108,* 8806-8816.

[23] S. Liu, R. Sang, S. Hong, Y. Cai, H. Wang, *Langmuir* **2013**, *29*, 8511-8516.

[24] M. J. L. Castro, J. Kovensky, A. F. Cirelli, *Langmuir* **2002**, *18,* 2477-2482.

[25] F. M. Menger, B. N. A. Mbadugha, *J. Am. Chem. Soc.* **2001**, *123,* 875-885.

[26] M. Johnsson, A. Wagenaar, M. C. A. Stuart, J. B. F. N. Engberts, *Langmuir* **2003**, *19,* 4609-4618.

[27] B. Obermeier, F. Wurm, C. Mangold, H. Frey, *Angew. Chem. Int. Ed*. **2011**, *50*, 7988-7997.

[28] S. Gupta, R. Tyagi, V. S. Parmar, S. K. Sharma, R. Haag, *Polymer* **2012**, *53*, 3053-3078.

[29] T. Zhou, H. Yang, X. Xu, X. Wang, J. Wang, G. Dong, *Colloids Surf. A* **2008***, 317, 339-343.*

[30] P. A. FitzGerald, T. W. Davey, G. G. Warr, *Langmuir* **2005**, *21,* 7121-7128.

[31] Z. Liwen, X. Honglu, *J. Disper. Sci. Technol*. **2008**, *29*, 284-288.

[32] H. C. Kim, E. Kim, T. L. Ha, S. W. Jeong, S. G. Lee, S. J. Lee, B. Lee, *Colloids Surf. B* **2015**, *127*, 206-212.

[33] H. C. Kim, E. Kim, S. G. Lee, S. J. Lee, H. Kim, S. W. Jeong, *J. Polym. Sci. A* **2014**, *52*, 582-589.

[34] H. Türk, A. Shukla, P. C. A. Rodrigues, H. Rehage, R. Haag, *Chem. Eur. J.* **2007**, *13*, 4187-4196.

[35] R. Zana, *Adv. Colloid Interface Sci*. **2002**, *97*, 205-253.

[36] S. Gupta, B. Schade, S. Kumar, C. Böttcher, S. K. Sharma, R. Haag, *Small* **2013**, *9,* 894-904.

[37] O. Saku, H. Ishida, E. Atsumi, Y. Sugimoto, H. Kodaira, Y. Kato, S. Shirakura, Y. Nakasato, *J. Med. Chem.* **2012**, *55*, 3436-3451.

[38] W. C. Griffin, *J. Soc. Cosmet. Chem.* **1949**, *1*, 311-326.

[39] K. Kalyanasundaram, J. K. Thomas, *J. Phys. Chem*. **1977**, *81*, 2176-2180.

[40] J. N. Israelachvili, D. J. Mitchell, B. W. Ninham, *J. Chem. Soc. Faraday Trans.* 2 **1976**, *72*, 1525-1568.

[41] J. N. Israelachvili, *Intermolecular and surface forces*, 3rd edn. Academic Press: *Boston*, 2011.

[42] K. Skrabania, A. Laschewsky, H. V. Berlepsch, C. Böttcher, Langmuir **2009**, *25*, 7594-7601.

[43] F. N. Padia, M. Yaseen, B. Gore, S. Rogers, G. Bell and J. R. Lu, *J. Phys. Chem. B* **2014**, *118*, 179-188.

[44] I. N. Kurniasih, H. Liang, S. Kumar, A. Mohr, S. K. Sharma, J. P. Rabe, R. Haag, *J. Mater. Chem. B* **2013**, 1, 3569-3577.

[45] G. M. Soliman, R. Sharma, A. O. Choi, S. K. Varshney, F. M. Winnik, A. K. Kakkar, D. Maysinger, *Biomaterials* **2010**, *31*, 8382-8392.

[46] B. N. S. Thota, H. V. Berlepsch, C. Böttcher, R. Haag, *Chem. Commun*. **2015**, *51*, 8648-8651.

[47] I. N. Kurniasih, H. Liang, J. P. Rabe, R. Haag, *Macromol. Rapid Commun*. **2010**, *31*, 1516-1520.

10.1002/asia.201700450

: **Entry for the Table of Contents**

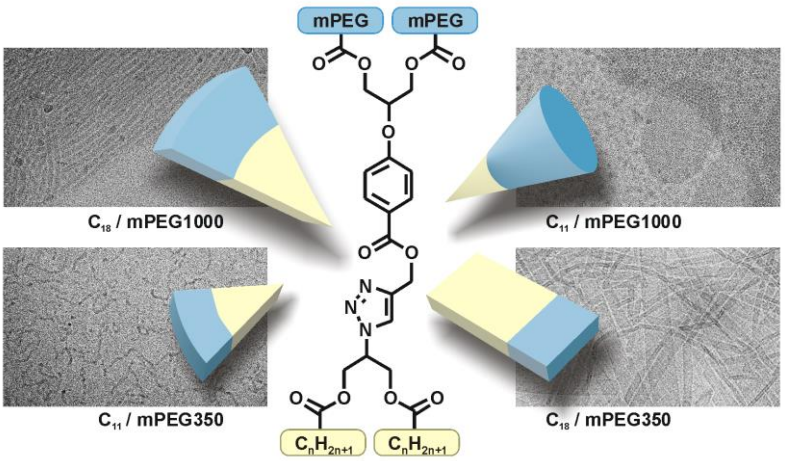

A new class of twinned amphiphiles was developed by utilizing 'Click chemistry' and acylation reactions on a chemo-enzymatically synthesized A_2B_2 monomer, the aggregation behaviour of these amphiphiles was investigated using fluorescence, DLS, cryo-TEM studies. The cryo-TEM measurements prove the formation of globular, thread-like or rod-like micelles as well as planar double-layer assemblies, depending on the amphiphile's molecular structure. The cytotoxicity study suggested the twinned amphiphiles to be suitable for in vivo applications. The transport capacity results for both Nimodipine and Nile Red prove them as a promising candidate for drug delivery.